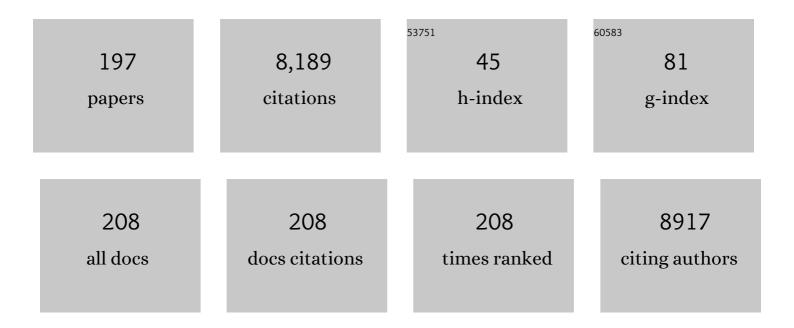
List of Publications by Year in descending order

Source: https://exaly.com/author-pdf/2868646/publications.pdf Version: 2024-02-01



#	Article	IF	CITATIONS
1	Honeycomb monolithic design to enhance the performance of Ni-based catalysts for dry reforming of methane. Catalysis Today, 2022, 383, 226-235.	2.2	8
2	New findings regarding the role of copper entity particle size on the performance of Cu/ceria-based catalysts in the CO-PROX reaction. Applied Surface Science, 2022, 575, 151717.	3.1	8
3	Segmentation of scanning-transmission electron microscopy images using the ordered median problem. European Journal of Operational Research, 2022, 302, 671-687.	3.5	5
4	Photocatalytic removal of benzene over Ti ₃ C ₂ T _{<i>x</i>} MXene and TiO ₂ –MXene composite materials under solar and NIR irradiation. Journal of Materials Chemistry C, 2022, 10, 626-639.	2.7	13
5	Microstructural and Chemical Investigations of Presolar Silicates from Diverse Stellar Environments. Astrophysical Journal, 2022, 925, 110.	1.6	4
6	Direct assessment of confinement effect in zeolite-encapsulated subnanometric metal species. Nature Communications, 2022, 13, 821.	5.8	30
7	Nanocrystalline BaCo ₃ (VO ₄) ₂ (OH) ₂ with a kagome lattice of Co(<scp>ii</scp>) ions: synthesis, crystal structure and magnetic properties. Journal of Materials Chemistry C, 2022, 10, 3287-3291.	2.7	4
8	Magneto-optical hyperthermia agents based on probiotic bacteria loaded with magnetic and gold nanoparticles. Nanoscale, 2022, 14, 5716-5724.	2.8	9
9	Encapsulation of Cynara Cardunculus Guaiane-type Lactones in Fully Organic Nanotubes Enhances Their Phytotoxic Properties. Journal of Agricultural and Food Chemistry, 2022, 70, 3644-3653.	2.4	7
10	Active and Regioselective Ru Single-Site Heterogeneous Catalysts for Alpha-Olefin Hydroformylation. ACS Catalysis, 2022, 12, 4182-4193.	5.5	17
11	Benzene and NO photocatalytic-assisted removal using indoor lighting conditions. Materials Today Energy, 2022, 25, 100974.	2.5	3
12	Low-Temperature Growth of Reactive Pyrochlore Nanostructures on Zirconia-Supported Ceria: Implications for Improved Catalytic Behavior. ACS Applied Nano Materials, 2022, 5, 6316-6326.	2.4	2
13	Quantitative Evaluation of Supported Catalysts Key Properties from Electron Tomography Studies: Assessing Accuracy Using Material-Realistic 3D-Models. Topics in Catalysis, 2022, 65, 859-870.	1.3	1
14	Improving the reducibility of CeO ₂ /TiO ₂ by high-temperature redox treatment: the key role of atomically thin CeO ₂ surface layers. Journal of Materials Chemistry A, 2022, 10, 13074-13087.	5.2	5
15	Graphene-TiO2 hybrids for photocatalytic aided removal of VOCs and nitrogen oxides from outdoor environment. Chemical Engineering Journal, 2021, 405, 126651.	6.6	90
16	3D-printing of metallic honeycomb monoliths as a doorway to a new generation of catalytic devices: the Ni-based catalysts in methane dry reforming showcase. Catalysis Communications, 2021, 148, 106181.	1.6	28
17	Tutorial: structural characterization of isolated metal atoms and subnanometric metal clusters in zeolites. Nature Protocols, 2021, 16, 1871-1906.	5.5	30
18	Cobalt nanoclusters coated with N-doped carbon for chemoselective nitroarene hydrogenation and tandem reactions in water. Green Chemistry, 2021, 23, 4490-4501.	4.6	31

#	Article	IF	CITATIONS
19	One-Step Encapsulation of <i>ortho</i> -Disulfides in Functionalized Zinc MOF. Enabling Metal–Organic Frameworks in Agriculture. ACS Applied Materials & Interfaces, 2021, 13, 7997-8005.	4.0	14
20	Cu O and carbon–modified TiO2–based hybrid materials for photocatalytically assisted H2 generation. Materials Today Energy, 2021, 19, 100607.	2.5	11
21	Tailoring the Transport Properties of Mesoporous Doped Cerium Oxide for Energy Applications. Journal of Physical Chemistry C, 2021, 125, 16451-16463.	1.5	5
22	Enhanced Artificial Enzyme Activities on the Reconstructed Sawtoothlike Nanofacets of Pure and Pr-Doped Ceria Nanocubes. ACS Applied Materials & Interfaces, 2021, 13, 38061-38073.	4.0	13
23	In-depth structural and analytical study of the washcoating layer of a Mn-Cu monolithic catalyst using STEM-FIB, EDX and EELS. Insights into stability under working conditions. Applied Surface Science, 2021, 563, 150318.	3.1	2
24	Nanostructure, compositional and magnetic studies of Poly(aniline)–CoFe2O4 nanocomposites. Nano Structures Nano Objects, 2021, 28, 100808.	1.9	3
25	Exceptional Low-Temperature CO Oxidation over Noble-Metal-Free Iron-Doped Hollandites: An In-Depth Analysis of the Influence of the Defect Structure on Catalytic Performance. ACS Catalysis, 2021, 11, 15026-15039.	5.5	5
26	Surface characterization of two Ce0.62Zr0.38O2 mixed oxides with different reducibility. Applied Surface Science, 2020, 503, 144255.	3.1	7
27	Atomic-level understanding on the evolution behavior of subnanometric Pt and Sn species during high-temperature treatments for generation of dense PtSn clusters in zeolites. Journal of Catalysis, 2020, 391, 11-24.	3.1	30
28	Optimization of STEMâ€HAADF Electron Tomography Reconstructions by Parameter Selection in Compressed Sensing Total Variation Minimizationâ€Based Algorithms. Particle and Particle Systems Characterization, 2020, 37, 2000070.	1.2	4
29	Photo-electrochemical properties of CuO–TiO ₂ heterojunctions for glucose sensing. Journal of Materials Chemistry C, 2020, 8, 9529-9539.	2.7	25
30	Cooperative and fully reversible color switching activation in hybrid graphene decorated nanocages and copper-TiO2 nanoparticles. Materials Today Energy, 2020, 17, 100460.	2.5	7
31	Structural modulation and direct measurement of subnanometric bimetallic PtSn clusters confined in zeolites. Nature Catalysis, 2020, 3, 628-638.	16.1	182
32	In-Depth Structural and Optical Analysis of Ce-modified ZnO Nanopowders with Enhanced Photocatalytic Activity Prepared by Microwave-Assisted Hydrothermal Method. Catalysts, 2020, 10, 551.	1.6	13
33	Unambiguous localization of titanium and iron cations in doped manganese hollandite nanowires. Chemical Communications, 2020, 56, 4812-4815.	2.2	6
34	Ultrathin Washcoat and Very Low Loading Monolithic Catalyst with Outstanding Activity and Stability in Dry Reforming of Methane. Nanomaterials, 2020, 10, 445.	1.9	8
35	Regioselective Generation of Single‣ite Iridium Atoms and Their Evolution into Stabilized Subnanometric Iridium Clusters in MWW Zeolite. Angewandte Chemie, 2020, 132, 15825-15832.	1.6	5
36	Regioselective Generation of Singleâ€6ite Iridium Atoms and Their Evolution into Stabilized Subnanometric Iridium Clusters in MWW Zeolite. Angewandte Chemie - International Edition, 2020, 59, 15695-15702.	7.2	46

#	Article	IF	CITATIONS
37	Quaternary LnxLa(1-x)S-TaS2 nanotubes (Ln=Pr, Sm, Ho, and Yb) as a vehicle for improving the yield of misfit nanotubes. Applied Materials Today, 2020, 19, 100581.	2.3	4
38	Optical and tomography studies of water-soluble gold nanoparticles on bacterial exopolysaccharides. Journal of Applied Physics, 2019, 126, 053101.	1.1	4
39	Enhanced UV emission of Li–Y co-doped ZnO thin films via spray pyrolysis. Journal of Alloys and Compounds, 2019, 808, 151710.	2.8	8
40	Regioselective generation and reactivity control of subnanometric platinum clusters in zeolites for high-temperature catalysis. Nature Materials, 2019, 18, 866-873.	13.3	339
41	Understanding the Complex Structure of CeO2/TiO2 Nanocatalyst. Key Contributions of the Combined Use of HAADF, X-EDS and EELS Spectroscopies. Microscopy and Microanalysis, 2019, 25, 578-579.	0.2	1
42	The Role of Goldâ€Alumina Template in the Electrochemical Deposition of CeO 2 Nanotubes. Particle and Particle Systems Characterization, 2019, 36, 1900168.	1.2	3
43	In Situ Eco Encapsulation of Bioactive Agrochemicals within Fully Organic Nanotubes. ACS Applied Materials & Interfaces, 2019, 11, 41925-41934.	4.0	13
44	HAADF-STEM Electron Tomography in Catalysis Research. Topics in Catalysis, 2019, 62, 808-821.	1.3	16
45	Influence of {111} nanofaceting on the dynamics of CO adsorption and oxidation over Au supported on CeO2 nanocubes: An operando DRIFT insight. Catalysis Today, 2019, 336, 90-98.	2.2	22
46	Accurate 3D Characterization of Catalytic Bodies Surface by Scanning Electron Microscopy. ChemCatChem, 2019, 11, 3171-3177.	1.8	4
47	Size, nanostructure, and composition dependence of bimetallic Au–Pd supported on ceria–zirconia mixed oxide catalysts for selective oxidation of benzyl alcohol. Journal of Catalysis, 2019, 375, 44-55.	3.1	43
48	Improving the Activity and Stability of YSZ-Supported Gold Powder Catalyst by Means of Ultrathin, Coherent, Ceria Overlayers. Atomic Scale Structural Insights. ACS Catalysis, 2019, 9, 5157-5170.	5.5	6
49	An atomically efficient, highly stable and redox active Ce0.5Tb0.5Ox (3% mol.)/MgO catalyst for total oxidation of methane. Journal of Materials Chemistry A, 2019, 7, 8993-9003.	5.2	12
50	Synergy of Neodymium and Copper for Fast and Reversible Visible-light Promoted Photochromism, and Photocatalysis, in Cu/Nd-TiO ₂ Nanoparticles. ACS Applied Energy Materials, 2019, 2, 3237-3252.	2.5	25
51	Selective oxidation of glycerol on morphology controlled ceria nanomaterials. Catalysis Science and Technology, 2019, 9, 2328-2334.	2.1	21
52	Catalytic Performance of Ni/CeO2/X-ZrO2 (X = Ca, Y) Catalysts in the Aqueous-Phase Reforming of Methanol. Nanomaterials, 2019, 9, 1582.	1.9	34
53	Influence of yttrium doping on the structural, morphological and optical properties of nanostructured ZnO thin films grown by spray pyrolysis. Ceramics International, 2019, 45, 6842-6852.	2.3	39
54	Apoferritin Protein Amyloid Fibrils with Tunable Chirality and Polymorphism. Journal of the American Chemical Society, 2019, 141, 1606-1613.	6.6	20

#	Article	IF	CITATIONS
55	Sunlight photoactivity of rice husks-derived biogenic silica. Catalysis Today, 2019, 328, 125-135.	2.2	21
56	Surface and redox characterization of new nanostructured ZrO ₂ @CeO ₂ systems with potential catalytic applications. Surface and Interface Analysis, 2018, 50, 1025-1029.	0.8	10
57	Synthesis of Densely Packaged, Ultrasmall Pt ⁰ ₂ Clusters within a Thioetherâ€Functionalized MOF: Catalytic Activity in Industrial Reactions at Low Temperature. Angewandte Chemie - International Edition, 2018, 57, 6186-6191.	7.2	115
58	A Macroscopically Relevant 3Dâ€Metrology Approach for Nanocatalysis Research. Particle and Particle Systems Characterization, 2018, 35, 1700343.	1.2	16
59	A Novel Electron Microscopic Characterization of Core/Shell Nanobiostimulator Against Parasitic Plants. ACS Applied Materials & amp; Interfaces, 2018, 10, 2354-2359.	4.0	12
60	Nanotubes from the Misfit Compound Alloy LaS-Nb _{<i>x</i>} Ta _(1–<i>x</i>) S ₂ . Chemistry of Materials, 2018, 30, 8829-8842.	3.2	11
61	Confined Pt ₁ ¹⁺ Water Clusters in a MOF Catalyze the Lowâ€Temperature Water–Gas Shift Reaction with both CO ₂ Oxygen Atoms Coming from Water. Angewandte Chemie - International Edition, 2018, 57, 17094-17099.	7.2	54
62	Selective Oxidation of Veratryl Alcohol over Au-Pd/Ce0.62Zr0.38O2 Catalysts Synthesized by Sol-Immobilization: Effect of Au:Pd Molar Ratio. Nanomaterials, 2018, 8, 669.	1.9	17
63	A single slice approach for simulating two-beam electron diffraction of nanocrystals. Ultramicroscopy, 2018, 195, 171-188.	0.8	2
64	Gradual Transformation of Ag ₂ S to Au ₂ S Nanoparticles by Sequential Cation Exchange Reactions: Binary, Ternary, and Hybrid Compositions. Chemistry of Materials, 2018, 30, 6893-6902.	3.2	12
65	Three-dimensional chemical mapping using non-destructive SEM and photogrammetry. Scientific Reports, 2018, 8, 11000.	1.6	8
66	Assessment of engineered surfaces roughness by high-resolution 3D SEM photogrammetry. Ultramicroscopy, 2017, 177, 106-114.	0.8	16
67	Synthesis of Supported Planar Iron Oxide Nanoparticles and Their Chemo- and Stereoselectivity for Hydrogenation of Alkynes. ACS Catalysis, 2017, 7, 3721-3729.	5.5	63
68	Improved Oxidase Mimetic Activity by Praseodymium Incorporation into Ceria Nanocubes. ACS Applied Materials & Interfaces, 2017, 9, 18595-18608.	4.0	71
69	Improving the Redox Response Stability of Ceria-Zirconia Nanocatalysts under Harsh Temperature Conditions. Chemistry of Materials, 2017, 29, 9340-9350.	3.2	21
70	Sub-nanometer surface chemistry and orbital hybridization in lanthanum-doped ceria nano-catalysts revealed by 3D electron microscopy. Scientific Reports, 2017, 7, 5406.	1.6	18
71	Highly stable ceria-zirconia-yttria supported Ni catalysts for syngas production by CO 2 reforming of methane. Applied Surface Science, 2017, 426, 864-873.	3.1	46
72	Critical Influence of Redox Pretreatments on the CO Oxidation Activity of BaFeO3â^'δ Perovskites: An in-Depth Atomic-Scale Analysis by Aberration-Corrected and in Situ Diffraction Techniques. ACS Catalysis, 2017, 7, 8653-8663.	5.5	13

#	Article	IF	CITATIONS
73	Combined Macroscopic, Nanoscopic, and Atomicâ€5cale Characterization of Gold–Ruthenium Bimetallic Catalysts for Octanol Oxidation. Particle and Particle Systems Characterization, 2016, 33, 419-437.	1.2	6
74	Effect of synthesis conditions on electrical and catalytical properties of perovskites with high value of A-site cation size mismatch. International Journal of Hydrogen Energy, 2016, 41, 19810-19818.	3.8	7
75	Strain Field in Ultrasmall Gold Nanoparticles Supported on Cerium-Based Mixed Oxides. Key Influence of the Support Redox State. Langmuir, 2016, 32, 4313-4322.	1.6	10
76	Synergistic effect of bimetallic Au-Pd supported on ceria-zirconia mixed oxide catalysts for selective oxidation of glycerol. Applied Catalysis B: Environmental, 2016, 197, 222-235.	10.8	62
77	CeO2-modified Au/TiO2 catalysts with outstanding stability under harsh CO oxidation conditions. Applied Catalysis B: Environmental, 2016, 197, 86-94.	10.8	25
78	Influence of pretreatment atmospheres on the performance of bimetallic Au-Pd supported on ceria-zirconia mixed oxide catalysts for benzyl alcohol oxidation. Applied Catalysis A: General, 2016, 525, 145-157.	2.2	35
79	CO Oxidation over Bimetallic Au–Pd Supported on Ceria–Zirconia Catalysts: Effects of Oxidation Temperature and Au:Pd Molar Ratio. Catalysis Letters, 2016, 146, 144-156.	1.4	29
80	Enhanced Hydroxyl Radical Scavenging Activity by Doping Lanthanum in Ceria Nanocubes. Journal of Physical Chemistry C, 2016, 120, 1891-1901.	1.5	77
81	A promoting effect of dilution of Pd sites due to gold surface segregation under reaction conditions on supported Pd–Au catalysts for the selective hydrogenation of 1,5-cyclooctadiene. Catalysis Today, 2016, 259, 213-221.	2.2	24
82	Lowâ€Lanthanideâ€Content CeO ₂ /MgO Catalysts with Outstandingly Stable Oxygen Storage Capacities: An Inâ€Depth Structural Characterization by Advanced STEM Techniques. ChemCatChem, 2015, 7, 3763-3778.	1.8	13
83	Comparative study of the catalytic performance and final surface structure of Co3O4/La-CeO2 washcoated ceramic and metallic honeycomb monoliths. Catalysis Today, 2015, 253, 190-198.	2.2	26
84	Ru-modified Au catalysts supported on ceria–zirconia for the selective oxidation of glycerol. Catalysis Today, 2015, 253, 178-189.	2.2	45
85	Critical Influence of Nanofaceting on the Preparation and Performance of Supported Gold Catalysts. ACS Catalysis, 2015, 5, 3504-3513.	5.5	53
86	Experimental evidences of the relationship between reducibility and micro- and nanostructure in commercial high surface area ceria. Applied Catalysis A: General, 2014, 479, 35-44.	2.2	13
87	Reversible deactivation of a Au/Ce0.62Zr0.38O2 catalyst in CO oxidation: A systematic study of CO2-triggered carbonate inhibition. Journal of Catalysis, 2014, 316, 210-218.	3.1	45
88	Speciation-controlled incipient wetness impregnation: A rational synthetic approach to prepare sub-nanosized and highly active ceria–zirconia supported gold catalysts. Journal of Catalysis, 2014, 318, 119-127.	3.1	20
89	UNDERSTANDING CERIA-BASED CATALYTIC MATERIALS: AN OVERVIEW OF RECENT PROGRESS. Catalytic Science Series, 2013, , 47-138.	0.6	2
90	The promotional effect of Sn-beta zeolites on platinum for the selective hydrogenation of	1.3	32

#	Article	IF	CITATIONS
91	Rational design of nanostructured, noble metal free, ceria–zirconia catalysts with outstanding low temperature oxygen storage capacity. Journal of Materials Chemistry A, 2013, 1, 4836.	5.2	42
92	Self-assembly of one-pot synthesized CexZr1â^'xO2–BaO·nAl2O3 nanocomposites promoted by site-selective doping of alumina with barium. Journal of Materials Chemistry A, 2013, 1, 3645.	5.2	12
93	Dramatic effect of redox pre-treatments on the CO oxidation activity of Au/Ce0.50Tb0.12Zr0.38O2â^'x catalysts prepared by deposition–precipitation with urea: a nano-analytical and nano-structural study. Chemical Communications, 2013, 49, 6722.	2.2	7
94	Combined (S)TEM-FIB Insight into the Influence of the Preparation Method on the Final Surface Structure of a Co ₃ O ₄ /La-Modified-CeO ₂ Washcoated Monolithic Catalyst. Journal of Physical Chemistry C, 2013, 117, 13028-13036.	1.5	13
95	Selective oxidative dehydrogenation of ethane over SnO2-promoted NiO catalysts. Journal of Catalysis, 2012, 295, 104-114.	3.1	87
96	Key insights on the structural characterization of textured Er2O3–ZrO2 nano-oxides prepared by a surfactant-free solvothermal route. Journal of Alloys and Compounds, 2012, 519, 29-36.	2.8	12
97	The role of Pd–Ga bimetallic particles in the bifunctional mechanism of selective methanol synthesis via CO2 hydrogenation on a Pd/Ga2O3 catalyst. Journal of Catalysis, 2012, 292, 90-98.	3.1	136
98	Imaging Nanostructural Modifications Induced by Electronic Metalâ^'Support Interaction Effects at Au Cerium-Based Oxide Nanointerfaces. ACS Nano, 2012, 6, 6812-6820.	7.3	29
99	Unknown Aspects of Self-Assembly of PbS Microscale Superstructures. ACS Nano, 2012, 6, 3800-3812.	7.3	92
100	Analysis and application of the theories that rationalize the crystalline structures of fluorite-related rare earth oxides. Catalysis Today, 2012, 180, 161-166.	2.2	0
101	A novel procedure for accurate estimations of the lattice parameter of supported nanoparticles from the analysis of plan view HREM images: Application to the structural investigation of Pd/CeO2 catalysts. Catalysis Today, 2012, 180, 174-183.	2.2	11
102	Synthesis of ceria-praseodimia nanotubes with high catalytic activity for CO oxidation. Catalysis Today, 2012, 180, 167-173.	2.2	26
103	SerafÃn Bernal: Profile of an excellent professor. Catalysis Today, 2012, 180, 1.	2.2	0
104	Structure transformations and reducibility of nanocrystalline Ce1â^'xYbxO2â^'(x/2) mixed oxides. Catalysis Today, 2012, 187, 56-64.	2.2	22
105	From synthetic to natural nanoparticles: monitoring the biodegradation of SPIO (P904) into ferritin by electron microscopy. Nanoscale, 2011, 3, 4597.	2.8	34
106	Magnetic Nanoparticles-Templated Assembly of Protein Subunits: A New Platform for Carbohydrate-Based MRI Nanoprobes. Journal of the American Chemical Society, 2011, 133, 4889-4895.	6.6	79
107	Recent Progress in Chemical Characterization of Supported Gold Catalysts: CO Adsorption on Au/Ceria–Zirconia. Chemistry Letters, 2011, 40, 1210-1216.	0.7	9
108	Advanced Electron Microscopy Investigation of Ceria–Zirconiaâ€Based Catalysts. ChemCatChem, 2011, 3, 1015-1027.	1.8	16

#	Article	IF	CITATIONS
109	CO Oxidation Activity of a Au/Ceria-Zirconia Catalyst Prepared by Deposition–Precipitation with Urea. Topics in Catalysis, 2011, 54, 931-940.	1.3	23
110	Chemical Imaging at Atomic Resolution as a Technique To Refine the Local Structure of Nanocrystals. Angewandte Chemie - International Edition, 2011, 50, 868-872.	7.2	27
111	Influence of the Preparation Procedure on the Catalytic Activity of Gold Supported on Diamond Nanoparticles for Phenol Peroxidation. Chemistry - A European Journal, 2011, 17, 9494-9502.	1.7	44
112	Nano-structural investigation of Ag/Al2O3 catalyst for selective removal of O2 with excess H2 in the presence of C2H4. Applied Catalysis A: General, 2011, 391, 187-193.	2.2	21
113	A Bioinspired Approach to the Synthesis of Bimetallic CoNi Nanoparticles. Inorganic Chemistry, 2010, 49, 1705-1711.	1.9	23
114	Influence of the calcination temperature on the nano-structural properties, surface basicity, and catalytic behavior of alumina-supported lanthana samples. Journal of Catalysis, 2010, 272, 121-130.	3.1	81
115	Contributions of Electron Microscopy to Understanding CO Adsorption on Powder Au/Ceria–Zirconia Catalysts. Chemistry - A European Journal, 2010, 16, 9536-9543.	1.7	16
116	Bridging the Gap between CO Adsorption Studies on Gold Model Surfaces and Supported Nanoparticles. Angewandte Chemie - International Edition, 2010, 49, 1981-1985.	7.2	35
117	Fully Reversible Metal Deactivation Effects in Gold/Ceria–Zirconia Catalysts: Role of the Redox State of the Support. Angewandte Chemie - International Edition, 2010, 49, 9744-9748.	7.2	42
118	Tuning operational conditions for efficient NOx storage and reduction over a Pt–Ba/Al2O3 monolith catalyst. Applied Catalysis B: Environmental, 2010, 96, 329-337.	10.8	26
119	Electron Microscopy Investigations of Nanostructured Ce/Mn Oxides for Catalytic Wet Oxidation. Journal of Physical Chemistry C, 2010, 114, 8981-8991.	1.5	16
120	Direct sub-nanometer scale electron microscopy analysis of anion incorporation to self-ordered anodic alumina layers. Corrosion Science, 2010, 52, 3763-3773.	3.0	26
121	Nanoparticles of Pd on Hybrid Polyoxometalateâ^'lonic Liquid Material: Synthesis, Characterization, and Catalytic Activity for Heck Reaction. Journal of Physical Chemistry C, 2010, 114, 8828-8836.	1.5	54
122	Selective hydrogenation of nitrocyclohexane to cyclohexanone oxime with H2 on decorated Pt nanoparticles. Journal of Catalysis, 2009, 263, 328-334.	3.1	49
123	3 D Characterization of Gold Nanoparticles Supported on Heavy Metal Oxide Catalysts by HAADF TEM Electron Tomography. Angewandte Chemie - International Edition, 2009, 48, 5313-5315.	7.2	72
124	Comparative study of the reducibility under H2 and CO of two thermally aged Ce0.62Zr0.38O2 mixed oxide samples. Catalysis Today, 2009, 141, 409-414.	2.2	27
125	Scanning Transmission Electron Microscopy Investigation of Differences in the High Temperature Redox Deactivation Behavior of CePrOx Particles Supported on Modified Alumina. Chemistry of Materials, 2009, 21, 1035-1045.	3.2	18
126	Single-Step Process To Prepare CeO ₂ Nanotubes with Improved Catalytic Activity. Nano Letters, 2009, 9, 1395-1400.	4.5	113

#	Article	IF	CITATIONS
127	Actual constitution of the mixed oxide promoter in a Rh/Ce1â^'xPrxO2â^'y/Al2O3 catalyst. Evolution throughout the preparation steps. Surface and Interface Analysis, 2008, 40, 242-245.	0.8	8
128	Quantum Dots Decorated with Magnetic Bionanoparticles. Advanced Functional Materials, 2008, 18, 3931-3935.	7.8	34
129	First Stage of Thermal Aging under Oxidizing Conditions of a Ce _{0.62} Zr _{0.38} O ₂ Mixed Oxide with an Ordered Cationic Sublattice: A Chemical, Nanostructural, and Nanoanalytical Study. Chemistry of Materials, 2008, 20, 5107-5113.	3.2	37
130	Transforming Nonselective into Chemoselective Metal Catalysts for the Hydrogenation of Substituted Nitroaromatics. Journal of the American Chemical Society, 2008, 130, 8748-8753.	6.6	496
131	Some recent results on the correlation of nano-structural and redox properties in ceria-zirconia mixed oxides. Journal of Alloys and Compounds, 2008, 451, 521-525.	2.8	32
132	Comparative Structural and Chemical Studies of Ferritin Cores with Gradual Removal of their Iron Contents. Journal of the American Chemical Society, 2008, 130, 8062-8068.	6.6	134
133	Preparation of Rhodium/Ce <i>_x</i> Pr ₁₋ <i>_x</i> O ₂ Catalysts:  A Nanostructural and Nanoanalytical Investigation of Surface Modifications by Transmission and Scanning-Transmission Electron Microscopy. Journal of Physical Chemistry C, 2008, 112. 5900-5910.	1.5	11
134	Looking at the surface of catalysts nanopowders. , 2008, , 183-184.		0
135	Structural Surface Investigations of Ceriumâ^'Zirconium Mixed Oxide Nanocrystals with Enhanced Reducibility. Journal of Physical Chemistry C, 2007, 111, 9001-9004.	1.5	36
136	Hydrogen Interaction with a Ceriaâ ''Zirconia Supported Gold Catalyst. Influence of CO Co-adsorption and Pretreatment Conditions. Journal of Physical Chemistry C, 2007, 111, 14371-14379.	1.5	65
137	Gold Nanoparticles in Organic Capsules: A Supramolecular Assembly of Gold Nanoparticles and Cucurbituril. Chemistry - A European Journal, 2007, 13, 6359-6364.	1.7	78
138	Increasing the Number of Oxygen Vacancies on TiO ₂ by Doping with Iron Increases the Activity of Supported Gold for CO Oxidation. Chemistry - A European Journal, 2007, 13, 7771-7779.	1.7	152
139	Sizeâ€Controlled Waterâ€Soluble Ag Nanoparticles. European Journal of Inorganic Chemistry, 2007, 2007, 4823-4826.	1.0	41
140	Redox Behavior of Thermally Aged Ceriaâ^'Zirconia Mixed Oxides. Role of Their Surface and Bulk Structural Properties. Chemistry of Materials, 2006, 18, 2750-2757.	3.2	63
141	Some major aspects of the chemical behavior of rare earth oxides: An overview. Journal of Alloys and Compounds, 2006, 408-412, 496-502.	2.8	39
142	TEM Investigation of the Synthesis of Rh/CePrOx Catalysts. Microscopy and Microanalysis, 2006, 12, 760-761.	0.2	1
143	TEM (HREM) and STEM (HAADF/EDS) Study of the Metallic Dispersion in Supported Ruthenium Catalysts. Microscopy and Microanalysis, 2006, 12, 810-811.	0.2	0
144	Model bimetallic Pd-Ni automotive exhaust catalysts: Influence of thermal aging and hydrocarbon self-poisoning. Applied Catalysis B: Environmental, 2006, 62, 359-368.	10.8	44

#	Article	IF	CITATIONS
145	Preparation of nickel(0) nanoparticles by arene-catalysed reduction of different nickel chloride-containing systems. Journal of Experimental Nanoscience, 2006, 1, 419-433.	1.3	23
146	A New Straightforward and Mild Preparation of Nickel(0) Nanoparticles. Chemistry Letters, 2005, 34, 1262-1263.	0.7	37
147	Synthesis of acidic Al-MCM-48: influence of the Si/Al ratio, degree of the surfactant hydroxyl exchange, and post-treatment in NHF solution. Journal of Catalysis, 2005, 230, 327-338.	3.1	75
148	Interaction of Pt and Rh nanoparticles with ceria supports: Ring opening of methylcyclobutane and CO hydrogenation after reduction at 373–723K. Applied Catalysis A: General, 2005, 294, 279-289.	2.2	19
149	ELECTRON MICROSCOPY IN THE CATALYSIS OF ALKANE OXIDATION, ENVIRONMENTAL CONTROL, AND ALTERNATIVE ENERGY SOURCES. Annual Review of Materials Research, 2005, 35, 465-504.	4.3	23
150	Combined HREM and HAADF Scanning Transmission Electron Microscopy:Â A Powerful Tool for Investigating Structural Changes in Thermally Aged Ceriaâ^'Zirconia Mixed Oxides. Chemistry of Materials, 2005, 17, 4282-4285.	3.2	35
151	Characterisation of Three-Way Automotive Aftertreatment Catalysts and Related Model Systems. Topics in Catalysis, 2004, 28, 31-45.	1.3	67
152	Thermal Stabilization of CexZr1-xO2Oxygen Storage Promoters by Addition of Al2O3:Â Effect of Thermal Aging on Textural, Structural, and Morphological Properties. Chemistry of Materials, 2004, 16, 4273-4285.	3.2	78
153	Nano-Scale Characterisation of Supported Phases in Catalytic Materials by High Resolution Transmission Electron Microscopy. Nanostructure Science and Technology, 2004, , 403-426.	0.1	5
154	Some contributions of electron microscopy to the characterisation of the strong metal–support interaction effect. Catalysis Today, 2003, 77, 385-406.	2.2	181
155	Structural, Morphological, and Oxygen Handling Properties of Nanosized Ceriumâ^'Terbium Mixed Oxides Prepared by Microemulsion. Chemistry of Materials, 2003, 15, 4309-4316.	3.2	81
156	In situ transmission electron microscopy investigation of Ce(iv) and Pr(iv) reducibility in a Rh (1%)/Ce0.8Pr0.2O2–x catalyst. Chemical Communications, 2003, , 644-645.	2.2	30
157	Optimization of tin dioxide nanosticks faceting for the improvement of palladium nanocluster epitaxy. Applied Physics Letters, 2002, 80, 329-331.	1.5	70
158	CHEMICAL AND NANOSTRUCTURAL ASPECTS OF THE PREPARATION AND CHARACTERISATION OF CERIA AND CERIA-BASED MIXED OXIDE-SUPPORTED METAL CATALYSTS. Catalytic Science Series, 2002, , 85-168.	0.6	25
159	Study of the Structural Modifications Induced by Reducing Treatments on a Pd/Ce0.8Tb0.2O2-x/La2O3â^'Al2O3Catalyst by Means of X-ray Diffraction and Electron Microscopy Techniques. Chemistry of Materials, 2002, 14, 1405-1410.	3.2	17
160	Computer image HRTEM simulation of catalytic nanoclusters on semiconductor gas sensor materials supports. Materials Science and Engineering B: Solid-State Materials for Advanced Technology, 2002, 91-92, 534-536.	1.7	5
161	Alumina- and Alumina–Zirconia-Supported PtSn Bimetallics: Microstructure and Performance for the n-Butane ODH Reaction. Journal of Catalysis, 2002, 208, 467-478.	3.1	40

162 Title is missing!. Catalysis Letters, 2001, 76, 131-137.

1.4 27

#	Article	IF	CITATIONS
163	Chlorine mobility in Pt/Al2O3 and Pt/Al2O3/Al complete oxidation catalysts Studies in Surface Science and Catalysis, 2001, 138, 413-420.	1.5	4
164	Surface structure and methylcyclobutane hydrogenolysis activity of Pt/Al2O3 and Pt/CeO2 after reduction at increasing temperature (373 to 973 K). Studies in Surface Science and Catalysis, 2000, 130, 2021-2026.	1.5	7
165	Structure of highly dispersed metals and oxides: exploring the capabilities of high-resolution electron microscopy. Surface and Interface Analysis, 2000, 29, 411-421.	0.8	35
166	Some recent results on metal/support interaction effects in NM/CeO2 (NM: noble metal) catalysts. Catalysis Today, 1999, 50, 175-206.	2.2	437
167	Textural and phase stability of CexZr1â^'xO2 mixed oxides under high temperature oxidising conditions. Catalysis Today, 1999, 50, 271-284.	2.2	105
168	Nanostructural evolution of high loading Rh/lanthana catalysts through the preparation and reduction steps. Catalysis Today, 1999, 52, 29-43.	2.2	19
169	Rare-earth oxides with fluorite-related structures: their systematic investigation using HREM images, image simulations and electron diffraction pattern simulations. Ultramicroscopy, 1999, 80, 19-39.	0.8	25
170	Structural characterisation of a VMgO catalyst used in the oxidative dehydrogenation of propane. Catalysis Letters, 1999, 57, 121-128.	1.4	42
171	Nanostructural Evolution under Reducing Conditions of a Pt/CeTbOxCatalyst:Â A New Alternative System as a TWC Component. Chemistry of Materials, 1999, 11, 3610-3619.	3.2	25
172	Image simulation and experimental HREM study of the metal dispersion in Rh/CeO2 catalysts. Influence of the reduction/reoxidation conditions. Applied Catalysis B: Environmental, 1998, 16, 127-138.	10.8	50
173	The interpretation of HREM images of supported metal catalysts using image simulation: profile view images. Ultramicroscopy, 1998, 72, 135-164.	0.8	154
174	Lanthanide compounds as environmentally-friendly corrosion inhibitors of aluminium alloys: a review. Corrosion Science, 1998, 40, 1803-1819.	3.0	453
175	Influence of the preparation procedure on the chemical and microstructural properties of lanthana promoted Rh/SiO2 catalysts. Journal of Alloys and Compounds, 1997, 250, 461-466.	2.8	18
176	Nanostructural Evolution of a Pt/CeO2Catalyst Reduced at Increasing Temperatures (473–1223 K): A HREM Study. Journal of Catalysis, 1997, 169, 510-515.	3.1	74
177	High-resolution electron microscopy investigation of metal–support interactions in Rh/TiO2. Journal of the Chemical Society, Faraday Transactions, 1996, 92, 2799-2809.	1.7	86
178	HREM study of the behaviour of a Rh/CeO2 catalyst under high temperature reducing and oxidizing conditions. Catalysis Today, 1995, 23, 219-250.	2.2	134
179	Lanthanide salts as alternative corrosion inhibitors. Journal of Alloys and Compounds, 1995, 225, 638-641.	2.8	57
180	The terbium oxide as support of highly dispersed metals. Study of the Rh/TbOx catalytic system. Journal of Alloys and Compounds, 1995, 225, 633-637.	2.8	5

#	Article	IF	CITATIONS
181	Comments on "Redox Processes on Pure Ceria and Rh/CeO2 Catalyst Monitored by X-ray Absorption (Fast Acquisition Mode). The Journal of Physical Chemistry, 1995, 99, 11794-11796.	2.9	58
182	Synthesis, characterization and performance of sol-gel prepared TiO2-SiO2catalysts and supports. Studies in Surface Science and Catalysis, 1995, , 461-470.	1.5	9
183	Influence of the nature of the metal precursor salt on the redox behaviour of ceria in Rh/CeO2 catalysts. Studies in Surface Science and Catalysis, 1995, 96, 419-429.	1.5	34
184	HRTEM and TPO Study of the Behaviour under Oxidizing Conditions of some Rh/CeO2 Catalysts. Studies in Surface Science and Catalysis, 1994, 82, 507-514.	1.5	24
185	Study of the COCeO2 interaction in presence of highly dispersed rhodium. Journal of Molecular Catalysis, 1994, 89, 391-396.	1.2	14
186	Influence of the Reduction/Evacuation Conditions on the Rate of Hydrogen Spillover on Rh/CeO2 Catalysts. Langmuir, 1994, 10, 717-722.	1.6	76
187	Characterization of silica dispersed lanthana by CO2 adsorption. Journal of Alloys and Compounds, 1994, 207-208, 201-205.	2.8	5
188	Microstructure and catalytic properties of Rh and Ni dispersed on TiO2-SiO2 aerogels. Journal of Sol-Gel Science and Technology, 1994, 2, 831-836.	1.1	9
189	Metal-support interaction phenomena in rhodium/ceria and rhodium/titania catalysts: Comparative study by high-resolution transmission electron spectroscopy. Applied Catalysis A: General, 1993, 99, 1-8.	2.2	46
190	Ultrasound as a tool for the preparation of gels: effect on the textural properties of TiO2-SiO2 aerogels. Journal of Materials Science, 1993, 28, 2191-2195.	1.7	16
191	Hydrogen chemisorption on ceria: influence of the oxide surface area and degree of reduction. Journal of the Chemical Society, Faraday Transactions, 1993, 89, 3499.	1.7	138
192	Microstructural and chemical properties of ceria-supported rhodium catalysts reduced at 773 K. The Journal of Physical Chemistry, 1993, 97, 4118-4123.	2.9	108
193	Preparation of rhodium catalysts dispersed on TiO2SiO2 aerogels. Journal of Non-Crystalline Solids, 1992, 147-148, 758-763.	1.5	30
194	Preparation and characterization of a praseodymium oxide to be used as a catalytic support. Journal of Alloys and Compounds, 1992, 180, 271-279.	2.8	31
195	Catalytic behaviour and surface properties of supported lanthana. Journal of Alloys and Compounds, 1992, 180, 295-301.	2.8	7
196	The key role of highly dispersed rhodium in the chemistry of hydrogen–ceria systems. Journal of the Chemical Society Chemical Communications, 1992, , 460-462.	2.0	30
197	HREM characterization of metal catalysts supported on rare-earth oxides: samarium oxide as support. Ultramicroscopy, 1990, 34, 60-65.	0.8	18